

# Incommensurate magnetic ordering in $\text{Cu}_2\text{Te}_2\text{O}_5\text{X}_2$ ( $X=\text{Cl},\text{Br}$ ) studied by single crystal neutron diffraction

O. Zaharko,\* H. Rønnow, and J. Mesot

*Laboratory for Neutron Scattering, ETHZ & PSI, CH-5232 Villigen, Switzerland*

S. J. Crowe and D. McK. Paul

*Department of Physics, University of Warwick, Coventry CV4 7AL, United Kingdom*

P. J. Brown

*Institut Laue-Langevin, 156X, 38042 Grenoble Cédex, France*

A. Daoud-Aladine

*ISIS Facility, Rutherford Appleton Laboratory, Chilton, Didcot, Oxfordshire OX10 0QX, United Kingdom*

A. Meents and A. Wagner

*Paul Scherrer Institute, CH-5232 Villigen, Switzerland*

M. Prester

*Institute of Physics, P.O. Box 304, HR-10 000, Zagreb, Croatia*

H. Berger

*Institut de Physique de la Matière Complexe, EPFL, CH-1015 Lausanne, Switzerland*

(Received 7 November 2005; revised manuscript received 10 January 2006; published 22 February 2006)

Polarized and unpolarized neutron-diffraction studies have been carried out on single crystals of the coupled spin tetrahedra systems  $\text{Cu}_2\text{Te}_2\text{O}_5\text{X}_2$  ( $X=\text{Cl},\text{Br}$ ). A model of the magnetic structure associated with the propagation vectors  $\mathbf{k}'_{\text{Cl}} \approx (-0.150, 0.422, \frac{1}{2})$  and  $\mathbf{k}'_{\text{Br}} \approx (-0.172, 0.356, \frac{1}{2})$  and stable below  $T_N=18$  K for  $X=\text{Cl}$  and  $T_N=11$  K for  $X=\text{Br}$  is proposed. A feature of the model, common to both the bromide and chloride, is a canted coplanar motif for the four  $\text{Cu}^{2+}$  spins on each tetrahedron which rotates on a helix from cell to cell following the propagation vector. The  $\text{Cu}^{2+}$  magnetic moment determined for  $X=\text{Br}$ ,  $0.395(5)\mu_B$ , is significantly less than for  $X=\text{Cl}$ ,  $0.88(1)\mu_B$  at 2 K. The magnetic structure of the chloride associated with the wave vector  $\mathbf{k}'$  differs from that determined previously for the wave vector  $\mathbf{k} \approx (0.150, 0.422, \frac{1}{2})$  [O. Zaharko *et al.*, Phys. Rev. Lett. **93**, 217206(E) (2004)].

DOI: [10.1103/PhysRevB.73.064422](https://doi.org/10.1103/PhysRevB.73.064422)

PACS number(s): 75.30.-m, 61.12.Ld, 75.10.Jm

## I. INTRODUCTION

Systems with weakly interacting frustrated magnetic clusters form an interesting class of materials with properties lying between those of quantum spin systems and classical magnets.<sup>1</sup> In this context the  $\text{Cu}_2\text{Te}_2\text{O}_5\text{X}_2$  ( $X=\text{Cl},\text{Br}$ ) (Ref. 2) compounds have recently attracted strong interest, as they contain  $\text{Cu}^{2+}$  tetrahedral clusters. The antiferromagnetic exchange interactions between the spins within a tetrahedron are geometrically frustrated and the coupling between the tetrahedra was assumed to be weak. Whilst the excitation spectrum of isolated tetrahedra is well known to be gapped, the presence of even small anisotropy or intertetrahedral coupling may lead to interesting new ground states and excitations. In these compounds the magnetic susceptibility reaches a maxima at  $T \sim 25$  K before dropping sharply at low temperatures, which was attributed to the presence of a singlet-triplet spin gap.<sup>2,3</sup> Further evidence of spin-gapped behavior in the bromide is observed in Raman scattering,<sup>3-5</sup> which also reveals evidence of what is suggested to be a low-energy longitudinal magnon. Fitting the susceptibility

data to an isolated tetrahedral model with four nearest-neighbor ( $J_1$ ) and two next-nearest-neighbor ( $J_2$ ) exchange interactions gives the coupling strengths  $J_1=J_2 \sim 43$  and  $38.5$  K for  $X=\text{Br}$  and  $\text{Cl}$ , respectively. However, susceptibility,<sup>2,3</sup> heat capacity<sup>3,5</sup> and thermal conductivity<sup>6,7</sup> measurements all show evidence of magnetic ordering at low temperatures,  $T_N=18$  K ( $\text{Cl}$ ) and  $11$  K ( $\text{Br}$ ), which requires intertetrahedral couplings. The effect of intertetrahedral coupling and the relative strengths of exchange interactions in this system have been investigated theoretically by band structure calculations,<sup>8</sup> spin dimer analysis,<sup>9</sup> flow-equation method,<sup>10</sup> and a mean field analysis.<sup>4,5</sup> The consequences of antisymmetric Dzyaloshinsky-Moriya (DM) interactions have been also analyzed.<sup>11</sup> Experimentally, magnetic excitations with a dispersive component are observed in both compounds by inelastic neutron scattering measurements,<sup>12,13</sup> which are associated with the development of long-range order.

The ground-state magnetic structure is found from neutron-diffraction studies to be rather complex.<sup>14</sup> Both compounds have incommensurate magnetic structures with wave

vectors  $\mathbf{k}'_{\text{Cl}} \approx (-0.150, 0.422, \frac{1}{2})$  and  $\mathbf{k}'_{\text{Br}} \approx (-0.172, 0.356, \frac{1}{2})$ . For  $\text{Cu}_2\text{Te}_2\text{O}_5\text{Cl}_2$  the coexistence of two different magnetic structures with  $\mathbf{k}' = (-k_x, k_y, \frac{1}{2})$  and  $\mathbf{k} = (k_x, k_y, \frac{1}{2})$  has been detected. In the model proposed for the  $\mathbf{k}$  structure the four  $\text{Cu}^{2+}$  ions of each tetrahedron form two pairs with the spins on the two ions of a pair rotating in the same plane with a constant canting angle between them. The canting angles were determined as  $38(6)^\circ$  for the first and  $111(10)^\circ$  for the second pair.

## II. NEW DIFFRACTION RESULTS

To obtain a more complete picture of the ground states of  $\text{Cu}_2\text{Te}_2\text{O}_5\text{X}_2$  we have made several new diffraction experiments. An x-ray diffraction experiment was carried out on a  $\text{Cu}_2\text{Te}_2\text{O}_5\text{Cl}_2$  single crystal ( $10 \mu\text{m}^3$ ) at 10 and 25 K at the X10 beamline ( $\lambda = 0.71073 \text{ \AA}$ ) at the SLS synchrotron. It revealed that the crystal structure of  $\text{Cu}_2\text{Te}_2\text{O}_5\text{Cl}_2$  at temperatures below and above  $T_N$ , has the same tetragonal space group  $P\bar{4}$ , as it does at 300 K.<sup>2</sup> The group is noncentrosymmetric and racemic twins were found to be present with the volume ratio 37(4):63(4). No features which could explain the coexistence of wave vectors  $\mathbf{k}$  and  $\mathbf{k}'$  below  $T_N$  were detected. The possibility of growth twins related by reflection in 100 planes was considered. No evidence for such twinning was obtained in the structure refinements confirming that the  $\{hkl\}$  and  $\{-kh\}$  families of reflections are independent.

Spherical neutron polarimetric measurements were made at 2 K on a  $\text{Cu}_2\text{Te}_2\text{O}_5\text{Cl}_2$  single crystal ( $6 \times 2.8 \times 2.6 \text{ mm}$ ) with CRYOPAD II installed on the D3 diffractometer at ILL ( $\lambda = 0.843 \text{ \AA}$ ). These were supplemented by unpolarized integrated intensity measurements at 2 K on the same  $\text{Cu}_2\text{Te}_2\text{O}_5\text{Cl}_2$  crystal and on a  $\text{Cu}_2\text{Te}_2\text{O}_5\text{Br}_2$  ( $4 \times 1 \times 1 \text{ mm}^3$ ) crystal using the D10 diffractometer at ILL ( $\lambda = 2.359 \text{ \AA}$ ).

The magnetic diffraction patterns given by the various  $\text{Cu}_2\text{Te}_2\text{O}_5\text{X}_2$  crystals studied so far show an important qualitative difference. The  $\text{Cu}_2\text{Te}_2\text{O}_5\text{Cl}_2$  crystal used in the present experiment gave four magnetic reflections at the lowest  $2\theta$  value (black spots in Fig. 1). They originate from two configuration domains with wave vectors  $\mathbf{k}'$  related by the fourfold axis (rotation of  $90^\circ$ ). For the  $\text{Cu}_2\text{Te}_2\text{O}_5\text{Br}_2$  crystal on the other hand only two reflections, corresponding to a single configuration domain, were found at the lowest angle (black spots connected by solid lines in Fig. 1). It should be recalled that in the previous study<sup>14</sup> eight reflections from two configuration domains of two independent wave vectors  $\mathbf{k}'$  and  $\mathbf{k}$  were reported (black and gray spots in Fig. 1).

There is a quantitative difference between the intensities of corresponding reflections obtained from the propagation vectors  $\mathbf{k}$  and  $\mathbf{k}'$ . This difference can be clearly seen by comparing the intensities  $I_1$  and  $I_2$  of the reflections  $000+\mathbf{k}$  and  $100-\mathbf{k}$ . For the  $\text{Cu}_2\text{Te}_2\text{O}_5\text{Cl}_2$  and  $\text{Cu}_2\text{Te}_2\text{O}_5\text{Br}_2$  crystals studied in the present experiment the inequality  $I_1 < I_2$  holds. In the previous study of another  $\text{Cu}_2\text{Te}_2\text{O}_5\text{Cl}_2$  crystal<sup>14</sup> this relation was the same  $I_1 < I_2$  for the  $\mathbf{k}'$  set, but opposite  $I_1 > I_2$  for the  $\mathbf{k}$  set; and it was from this latter set that the  $\mathbf{k}$  structure was derived.<sup>15</sup>

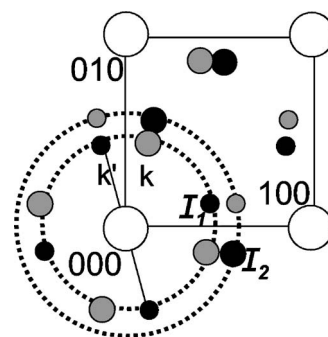


FIG. 1. The  $hk0$  and  $hk\frac{1}{2}$  layers of reciprocal space of a  $\text{Cu}_2\text{Te}_2\text{O}_5\text{X}_2$  crystal. Black circles correspond to magnetic reflections  $\{hk\frac{1}{2}\}$  of  $\mathbf{k}'$  and gray circles to those of  $\mathbf{k}$  wave vectors. The circle radii are proportional to intensities of magnetic reflections. Dashed circles with center at  $000$  connect reflections with intensity  $I_1$  and  $I_2$ .

In what follows we will describe the experimental observations made on wave vector  $\mathbf{k}'$  and will use them to derive a model for the  $\mathbf{k}'$  magnetic structure. For polarimetric measurements the crystal was mounted with the  $a^*$  direction vertical inside an ILL orange cryostat and cooled to 2 K. As the wave vector  $\mathbf{k}' \approx [-0.150, 0.422, \frac{1}{2}]$  has a small  $a^*$  component, the beam scattered by a magnetic reflection  $hkl$  with  $h=0.15$  is tilted from the horizontal plane by an angle  $\nu \approx 1^\circ$  and can be measured by ensuring that the vertical aperture of the detector is wide enough. The inclination  $\rho$  of the scattering vectors to the horizontal plane is  $\rho = 11.6^\circ$  for  $k=0.422, l=\frac{1}{2}$  and  $\rho = 4.6^\circ$  for  $k=0.422, l=\frac{3}{2}$ . The polarization of the scattered beam was measured using a spin polarized  $^3\text{He}$  filter. The filter polarization decayed with a time constant of  $\approx 100 \text{ h}$  and its effective polarization transmission varied from  $\sim 0.73$  to  $\sim 0.55$  between filter changes. The decay was followed by measuring the polarization scattered by the  $002$  nuclear reflection at regular intervals and an appropriate correction was applied to the scattered polarizations.

Measurements of each reflection were made with the incident neutrons polarized successively in three directions: parallel to the vertical  $z$  direction ( $P'_z$ ), along the  $x$  horizontal component of the scattering vector  $\mathbf{q}$  ( $P'_x$ ) and in the  $y$  direction that completes the right-handed Cartesian set. In this polarization coordinate system the magnetic interaction vector ( $\mathbf{M}_\perp = \mathbf{C} + i \cdot \mathbf{D}$ ), which is the projection of the Fourier transform of the magnetization  $\mathbf{M}(\mathbf{r})$  onto the plane perpendicular to  $\mathbf{q}$ , lies mainly in the  $yz$  plane. For each incident polarization direction the components of scattered polarization parallel to the  $x$ ,  $y$ , and  $z$  directions were determined. The six magnetic reflections labeled  $\mathbf{h}_1$ – $\mathbf{h}_6$  in Table I were studied. Their intensities were rather weak, and the background at low  $2\theta$  rather high, especially for the reflections  $\mathbf{h}_1$ ,  $\mathbf{h}_2$ ,  $\mathbf{h}_3$ , so reasonable statistics could only be obtained by measuring for about 6 h/reflection. Even a qualitative analysis of the scattered polarization sets a number of valuable constraints on possible models for the magnetic structure of  $\text{Cu}_2\text{Te}_2\text{O}_5\text{Cl}_2$ .

The polarization  $\mathbf{P}$  of neutrons scattered by a pure magnetic reflection can be written as:<sup>16,17</sup>

TABLE I. Polarization matrices  $P_{ij}$  measured for  $\mathbf{k}'$  magnetic reflections of  $\text{Cu}_2\text{Te}_2\text{O}_5\text{Cl}_2$  at 2 K ( $i$ : incoming,  $j$ : outgoing component of polarization).  $I$  is the measured intensity.

	$h k l$		$P'_i$	$P_{ix}$	$P_{iy}$	$P_{iz}$	$I$
$\mathbf{h}_1$	0.15 -0.42 $\frac{1}{2}$	$-x$		0.93(5)	-0.04(5)	0.19(4)	5.0(3)
		$y$		0.83(9)	-0.71(9)	0.03(8)	3.0(2)
		$z$		0.6(1)	-0.2(1)	1.0(1)	2.2(2)
$\mathbf{h}_2$	0.15 -0.42 $-\frac{1}{2}$	$-z$		1.2(1)	0.18(8)	-0.34(10)	2.2(2)
		$x$		0.93(8)	-0.03(9)	0.33(7)	4.5(2)
		$y$		0.8(2)	-0.5(2)	0.6(2)	2.7(1)
$\mathbf{h}_3$	-0.15 -0.58 $\frac{1}{2}$	$z$		0.7(2)	-0.0(2)	1.1(2)	2.3(1)
		$-z$		0.7(1)	-0.2(1)	-0.3(2)	3.1(4)
		$x$		-1.03(3)	-0.04(3)	0.27(3)	6.4(1)
$\mathbf{h}_4$	-0.15 0.42 $\frac{3}{2}$	$y$		-1.12(6)	-0.32(6)	-0.08(6)	3.6(1)
		$z$		-0.97(7)	-0.32(6)	0.55(6)	3.4(1)
		$-x$		-0.88(10)	-0.11(8)	0.16(8)	2.3(1)
$\mathbf{h}_5$	-0.15 0.42 $-\frac{3}{2}$	$x$		1.01(4)	0.06(4)	-0.16(4)	3.3(1)
		$y$		0.44(5)	-0.92(6)	-0.47(5)	3.9(1)
		$z$		0.56(5)	-0.40(4)	0.76(5)	3.8(4)
$\mathbf{h}_6$	0.15 -0.42 $\frac{3}{2}$	$-z$		0.24(6)	0.32(5)	-0.88(5)	3.8(3)
		$x$		-0.93(10)	0.03(8)	0.11(8)	2.0(3)
		$y$		0.52(6)	-0.73(6)	0.32(5)	3.0(4)
		$z$		0.54(6)	0.34(5)	0.88(6)	4.2(3)
		$x$		-0.92(6)	-0.10(6)	-0.27(4)	3.3(6)
		$y$		0.53(4)	-0.84(4)	-0.38(3)	4.4(1)
		$z$		0.43(4)	-0.61(3)	0.86(3)	3.4(2)

$$PI = -\mathbf{P}'(\mathbf{M}_\perp \cdot \mathbf{M}_\perp^*) + 2 \text{Re}[\mathbf{M}_\perp(\mathbf{P}' \cdot \mathbf{M}_\perp^*)] - 2 \text{Im}(\mathbf{M}_\perp \times \mathbf{M}_\perp^*) \quad (1)$$

with the first term parallel to  $\mathbf{P}'$ , the second to  $\mathbf{M}_\perp$ , and the third to  $\mathbf{q}$ .  $I$  is the scattered intensity which contains a polarization independent and a polarization dependent term

$$I = \mathbf{M}_\perp \cdot \mathbf{M}_\perp^* + \mathbf{P}' \cdot \text{Im}(\mathbf{M}_\perp \times \mathbf{M}_\perp^*). \quad (2)$$

These equations rewritten in the form of polarization matrices<sup>19</sup>

$$P_{ij} = \begin{pmatrix} -\frac{M^2 + J_{yz}}{M^2 + J_{yz}} & 0 & 0 \\ -\frac{J_{yz}}{M^2 + J_{yz}} & \frac{-M^2 + R_{yy}}{M^2} & \frac{R_{yz}}{M^2} \\ -\frac{J_{yz}}{M^2 + J_{yz}} & \frac{R_{yz}}{M^2} & \frac{-M^2 + R_{zz}}{M^2} \end{pmatrix} \quad (3)$$

with  $M^2 = \mathbf{M}_\perp \cdot \mathbf{M}_\perp^*$ ,  $R_{ij} = 2\text{Re}(M_{\perp i} M_{\perp j}^*)$  and  $J_{ij} = 2\text{Im}(M_{\perp i} M_{\perp j}^*)$  can be directly compared with the results presented in Table I.

Before attempting a detailed analysis, the different types of magnetic domains which can be present in  $\text{Cu}_2\text{Te}_2\text{O}_5\text{X}_2$  should be considered. It is worth remembering<sup>13</sup> that configuration, orientation and chiral magnetic domains are all

possible. The configuration domains give rise to separate sets of magnetic peaks and are not important for the polarization data analysis. Orientation domains can occur if the  $2_z$  axis is not in the magnetic symmetry group. Chirality domains are present because the propagation vector  $\mathbf{k}'$  is not one half of a reciprocal lattice vector ( $\mathbf{k}' \neq \mathbf{g} - \mathbf{k}'$ ). They are not the same as racemic twins which are allowed because the inversion center is missing in the crystallographic space group. The last two types of domain contribute to the same magnetic peaks and their presence could significantly complicate the D3 data analysis since orientation domains can depolarize the scattered beam and chirality domains can conceal the special features of helical structures. It was found that within the statistical accuracy the scattered beam was fully polarized for all measured reflections which suggests that only one orientation domain is present. The two chiral domains are also unequally populated, since the  $\mathbf{h}_1$  and  $\mathbf{h}_2$  reflections were almost absent for incident polarization  $P'_{+x}$ , but had significant intensity for  $P'_{-x}$ .

Furthermore, based on the polarization data we can immediately deduce the type of magnetic structure. The very presence of the  $x$  components in the scattered polarization ( $P_{yx}$  and  $P_{zx}$ ) indicates rotation of polarization towards  $\mathbf{q}$ , which is not compatible with any amplitude modulated or collinear structure. Such structures would have  $\mathbf{M}_\perp \parallel \mathbf{M}_\perp^*$  and the neutron polarization would only precess by  $180^\circ$  about  $\mathbf{M}_\perp$ . Therefore the magnetic structure must be helical.

The most significant qualitative conclusions from the polarimetric measurements are as follows.

(1) The scattered polarization for the reflection  $\mathbf{h}_2$  with  $\mathbf{q}_2 \parallel \mathbf{k}'$ , shows that the structure is not composed of helices with spins rotating in a plane normal to the wave vector  $\mathbf{k}'$ , for in such a case all polarization would be rotated towards the  $x$  direction. The presence of  $y$  and  $z$  components of scattered polarization indicates that one or more of the planes in which the spins rotate (plane of helices) must be inclined to the wave vector.

(2) For all the reflections studied the  $P_{zz}$  components are positive, while  $P_{yy}$  are negative. (i) This clearly indicates that all  $\mathbf{M}_\perp$  vectors have a  $z$  component, so there must be a component of the magnetic moment along  $a$ . (ii) It also means that the  $z$  components of  $\mathbf{M}_\perp$  are larger than the  $y$  components ( $C_z^2 + D_z^2 > C_y^2 + D_y^2$ ). This might indicate that the planes of the helices are close to or contain the  $a$  axis.

(3) The magnitude of the  $P_{yy}$  and  $P_{zz}$  components tend to be larger for reflections with  $l = \frac{3}{2}$  than for those with  $l = \frac{1}{2}$  which strongly suggests the existence of a  $c$  component of the magnetic moment.

Following the description of a magnetic structure given in reference,<sup>14</sup> we express the moment  $\mathbf{S}_{jl}$  of the  $j$ th  $\text{Cu}^{2+}$  ion in the  $l$ th unit cell as

$$\mathbf{S}_{jl} = \mathbf{A}_j \cos(\mathbf{k}' \cdot \mathbf{r}_l + \psi_j) + \mathbf{B}_j \sin(\mathbf{k}' \cdot \mathbf{r}_l + \psi_j) \quad (4)$$

with  $\mathbf{r}_l$  being the vector defining the origin of the  $l$ th unit cell.  $\mathbf{A}_j$  and  $\mathbf{B}_j$  are orthogonal vectors which determine the magnitude and direction of the helix associated with the  $j$ th ion, while  $\psi_j$  defines its phase. The four independent  $\text{Cu}^{2+}$  moments of the  $\text{Cu}_2\text{Te}_2\text{O}_5\text{Cl}_2$  unit cell could rotate on independent helices in which case it would be necessary to de-

TABLE II. Polarization matrices  $P_{ij}$  calculated for final model of the  $\mathbf{k}'$  magnetic structure of  $\text{Cu}_2\text{Te}_2\text{O}_5\text{Cl}_2$  presented in Table III.

	$h k l$	$P'_i$	$P_{ix}$	$P_{iy}$	$P_{iz}$	
$\mathbf{h}_1$	0.15 -0.42	$\frac{1}{2}$	$-x$	0.97	0.00	0.26
			$y$	0.83	-0.53	0.15
			$z$	0.64	-0.02	0.77
$\mathbf{h}_2$	0.15 -0.42	$-\frac{1}{2}$	$-x$	0.97	0.00	0.26
			$y$	0.83	-0.53	0.19
			$z$	0.64	0.03	0.77
$\mathbf{h}_3$	-0.15 -0.58	$\frac{1}{2}$	$x$	-0.94	-0.30	-0.13
			$y$	-0.98	-0.03	0.21
			$z$	-0.79	-0.34	0.50
$\mathbf{h}_4$	-0.15 0.42	$\frac{3}{2}$	$x$	-0.98	-0.06	0.19
			$-x$	0.99	0.03	-0.13
			$y$	0.38	-0.80	-0.47
$\mathbf{h}_5$	-0.15 0.42	$-\frac{3}{2}$	$x$	-0.98	0.06	0.19
			$y$	0.45	-0.80	0.40
			$z$	0.54	0.42	0.73
$\mathbf{h}_6$	0.15 -0.42	$\frac{3}{2}$	$x$	-0.98	0.06	-0.19
			$y$	0.45	-0.80	-0.40
			$z$	0.28	-0.45	0.85

fine the plane of each helix in polar coordinates by the angles  $\theta_j$ ,  $\phi_j$  of  $\mathbf{B}_j$ . There is freedom to choose the origin of each helix and a convenient choice is with the vector  $\mathbf{A}_j$  in the  $ab$  plane ( $\theta_{\mathbf{A}_j} = 90^\circ$ ). For the class of models in which the four  $\text{Cu}^{2+}$  ions rotate as two canted pairs<sup>14</sup> there are only two planes to define since the moments on the two ions of a pair rotate in the same one ( $\theta$ ,  $\phi$  are the same). The difference between the  $\psi$  values of the two ions is the canting angle for the pair  $\alpha$ .

Least-squares refinement of the  $\theta$ ,  $\phi$  and  $\psi$  parameters against the polarimetric measurements for the reflections  $\mathbf{h}_1$ – $\mathbf{h}_6$  made using a CCSL program<sup>18</sup> lead to the following conclusions.

(1) The data are sensitive to the difference between the  $\phi$  angles of the two helices which defines the angle between the two planes, and to the absolute value of  $\theta_{\mathbf{B}}$  which defines their inclination to the  $c$  axis. However, the sensitivity to the absolute values of the angle  $\phi$  which defines their inclination to the  $a$  axis and the phase  $\psi$  is not very high.

(2) The assumption that the envelope of the helices is circular ( $|\mathbf{A}_j| = |\mathbf{B}_j|$ ) and that all the  $\text{Cu}^{2+}$  ions have the same moment is supported by the polarimetric data. No significant improvement in the fit was obtained by allowing any of the components of moment to vary.

(3) The best agreement (Table II) was achieved for a model comprising two pairs of spins with the  $\mathbf{A}$  vectors lying in the  $ab$  plane ( $\theta_{\mathbf{A}} = 90^\circ$ ) and the  $\mathbf{B}$  vectors directed along the  $c$  axis ( $\theta_{\mathbf{B}} = 0^\circ$ ). The angle between the two planes on

TABLE III. The  $\mathbf{k}'$  magnetic structure of  $\text{Cu}_2\text{Te}_2\text{O}_5\text{X}_2$  ( $X = \text{Cl}, \text{Br}$ ). The origin of the helices is chosen in the  $ab$  plane ( $\theta_{\mathbf{A}} = 90^\circ$ ). The phase of the first helix  $\psi_1$  is set to  $0^\circ$ .  $\phi_{\mathbf{B}} = \phi_{\mathbf{A}} + 90^\circ$  due to orthogonality of  $\mathbf{A}_j$  and  $\mathbf{B}_j$ .  $\theta_{\mathbf{B}}$  is fixed to zero based on polarization data.  $\alpha_{ij}$  ( $i, j = 1, 4$ ) is the canting angle between moments of the  $\text{Cu}^{2+}$  ions with coordinates  $x \approx 0.730$ ,  $y \approx 0.453$ ,  $z \approx 0.158$ : 1 ( $x, y, z$ ), 2 ( $1-x, 1-y, z$ ), 3 ( $y, 1-x, -z$ ), 4 ( $1-y, x, -z$ ).

	$m$ ( $\mu_B/\text{Cu}$ )	$\phi_{\mathbf{A}}$	$\psi_2$	$\psi_3$	$\psi_4$ (deg.)	
$X = \text{Cl}$	0.88(1)	14(5)	13(3)	44(3)	-26(4)	
$X = \text{Br}$	0.395(5)	9(5)	22(4)	75(5)	-46(3)	
	$\alpha_{12}$	$\alpha_{34}$	$\alpha_{13}$	$\alpha_{14}$	$\alpha_{23}$	$\alpha_{24}$ (deg.)
$X = \text{Cl}$	13	70	135	154	147	142
$X = \text{Br}$	22	120	105	134	127	112

which the spin pairs rotate is small, not exceeding  $10^\circ$ . Allowing the four helices to be independent did not improve the fit.

(4) To fix other details of the magnetic structure we need to complement the polarimetric data with the integrated intensity measurements.

The unpolarized integrated intensity sets consist of 98  $\mathbf{k}'$  magnetic (and 286 nuclear) reflections for the  $\text{Cu}_2\text{Te}_2\text{O}_5\text{Cl}_2$  crystal and 44 magnetic (30 nuclear) for the  $\text{Cu}_2\text{Te}_2\text{O}_5\text{Br}_2$  crystal. Due to the small size of the  $\text{Cu}_2\text{Te}_2\text{O}_5\text{Br}_2$  crystal and its low magnetic moment, very long counting times were needed; measurement of each magnetic reflection lasted up to 4.5 h. Nuclear intensities were corrected for absorption and extinction, which for the  $\text{Cu}_2\text{Te}_2\text{O}_5\text{Cl}_2$  crystal was significant. When modeling the magnetic structure the scale refined from the nuclear reflections and the parameters reliably determined from the polarimetry experiment were fixed. We assumed a constant moment model and constrained  $\mathbf{A}$  to lie in the  $ab$  plane and  $\mathbf{B}$  to be parallel to the  $c$  axis. The intensity data are sensitive to the absolute values of the magnetic moment and the angles  $\phi_{\mathbf{A}}$  and  $\psi$ , in contrast to the polarimetric data, and the values obtained from these refinements are given in Table III. The model itself is illustrated schematically in Fig. 2. The goodness of fit of the model in which there was a difference in the  $\phi_{\mathbf{A}}$  angles of two pairs of  $10^\circ$  was not significantly different from that in which it was zero, so within the statistical accuracy all spins rotate in the same plane.

For  $\text{Cu}_2\text{Te}_2\text{O}_5\text{Br}_2$  the same constraints were used in the refinement of the integrated intensity data. The final values are listed in Table III and the structure is presented in Fig. 3. The refinement was much more stable than for the  $\text{Cu}_2\text{Te}_2\text{O}_5\text{Cl}_2$  intensity data and always converged to these final values, even when releasing the constraints and starting with different initial values. In fact, a simulated annealing algorithm<sup>21,22</sup> was applied to the generalized helix model (in which the moments are equal but all other constraints on the helices are relaxed), and the resulting structure was extremely close to that presented in Fig. 3.

The model for the  $\mathbf{k}'$  structure of  $\text{Cu}_2\text{Te}_2\text{O}_5\text{Cl}_2$  developed here gives a good fit to the limited  $\mathbf{k}'$  set of reflections mea-

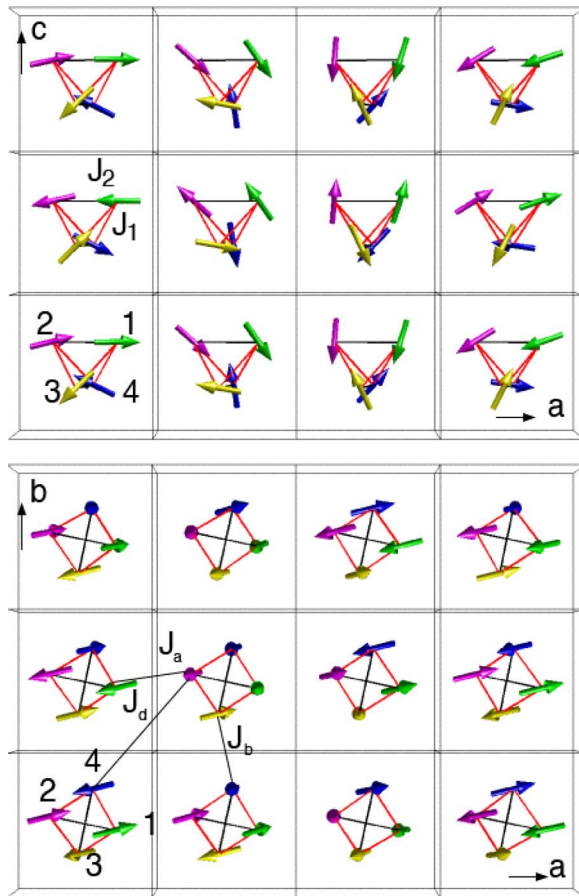


FIG. 2. (Color online) The  $ac$  (top) and  $ab$  (bottom) view on the layer of spin tetrahedra of the  $\text{Cu}_2\text{Te}_2\text{O}_5\text{Cl}_2$   $\mathbf{k}'$  magnetic structure. The origin is shifted by  $[0\ 0\ 1/2]$  relative to the crystallographic unit cell.

sured previously.<sup>14</sup> This model gives very poor agreement with the  $\mathbf{k}$  reflections, but significant improvement can be achieved by allowing the planes in which the two pairs rotate to be inclined to one another in accordance with the previously determined  $\mathbf{k}$  model. An interesting detail is that the canting angles  $\alpha_{12}$  and  $\alpha_{34}$  are almost the same in the  $\mathbf{k}'$   $X=\text{Cl}, \text{Br}$  and  $\mathbf{k}$   $X=\text{Cl}$  structures of  $\text{Cu}_2\text{Te}_2\text{O}_5X_2$ .

### III. DISCUSSION

The findings of our experiment, namely, the coexistence, in some crystals, of two symmetrically independent wave vectors  $\mathbf{k}'$  and  $\mathbf{k}$ ; two different magnetic structures, one associated with each wave vector; two different configurations for the spins in the  $\text{Cu}^{2+}$  tetrahedra: the “canted coplanar” and “canted pair” motifs in these magnetic structures, are very puzzling.

The ground state of an isolated tetrahedron with AF exchange interactions between  $S=1/2$  spins at the vertices is a singlet  $\sum_{i=1}^4 S_i=0$ . No long-range magnetic order would exist in a structure built from such isolated tetrahedra at any temperature. If the tetrahedra have tetragonal rather than cubic symmetry, as in the present case, there are two different intratetrahedral exchange constants: nearest-neighbor  $J_1$  and

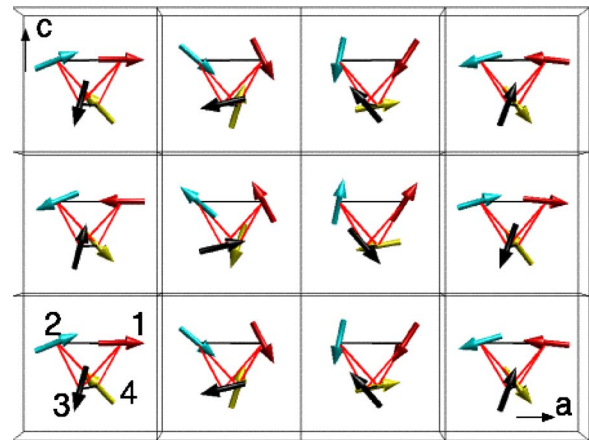


FIG. 3. (Color online) The  $ac$  layer of spin tetrahedra of the  $\text{Cu}_2\text{Te}_2\text{O}_5\text{Br}_2$   $\mathbf{k}'$  magnetic structure.

next-nearest-neighbor  $J_2$ . If  $J_1 > J_2$  the singlet state involves all four spins whereas if  $J_1 < J_2$  the spins form two dimers, each dimer individually forming a spin singlet.<sup>10</sup> In the  $\text{Cu}_2\text{Te}_2\text{O}_5X_2$  system due to strong intertetrahedral coupling the tetramers and dimers are not true singlets and the ground state is magnetically ordered.

The system is very complex and the ground-state spin arrangement is determined by competition between the geometrically frustrated intratetrahedral coupling, the exchange between tetrahedra and the antisymmetric Dzyaloshinski-Moriya interactions. It is possible that the interplay between these various couplings could result in several different but nearly degenerate spin configurations. In this case the spin system could be prompted to adopt one out of several possible arrangements by perturbations due to oxygen or copper defects associated with slight chemical inhomogeneity. This would explain why the coexistence of  $\mathbf{k}'$  and  $\mathbf{k}$  is strongly sample dependent. If we consider the lattice defined by the centers of the tetrahedra, ignoring their symmetry, another observation, the equality in the lengths of the components  $k_x$  and  $k_y$  for the  $\mathbf{k}'$  and  $\mathbf{k}$  wave vectors, becomes clear. Such a lattice has full tetragonal symmetry and the  $\mathbf{k}'$  and  $\mathbf{k}$  wave vectors are symmetrically equivalent. This could mean that the length of the wave vector is determined by the intertetrahedral exchange and until there is intratetrahedral ordering, the two wave vectors are degenerate. We suggest that the final arrangement adopted by the tetrahedra may be determined either by chance nucleation and growth of one rather than the other wave vector or by small alterations in the relative strengths of intratetrahedral interactions caused by crystal inhomogeneities.

The  $\mathbf{k}'$  structure is the one which occurs most frequently in the  $\text{Cu}_2\text{Te}_2\text{O}_5X_2$  crystals studied up to now by neutron diffraction. Its main feature is that the helices of all spins rotate almost in a single plane, which is close to (010). The four spins of each  $\text{Cu}^{2+}$  tetrahedron form a canted coplanar motif which rotates on a single helix with propagation vector  $\mathbf{k}'$ . The refined moment is  $0.88(1)\mu_B/\text{Cu}$  ( $X=\text{Cl}$ ) and  $0.395(5)\mu_B/\text{Cu}$  ( $X=\text{Br}$ ).

The angles between the spins on the sites 1-2 and 3-4 are very different from one another: the Cu1-Cu2 spins are al-

TABLE IV. Comparison between selected observed and calculated magnetic structure factors of  $\mathbf{k}'$  (present D10 experiment,  $F^{\mathbf{k}'}, h^{\mathbf{k}'}$ ) and  $\mathbf{k}$  (previous D15 experiment,  $F^{\mathbf{k}}, h^{\mathbf{k}}$ ) reflections of  $\text{Cu}_2\text{Te}_2\text{O}_5\text{Cl}_2$  crystals.

$h^{\mathbf{k}'}$	$k$	$l$	$F_{\text{obs}}^{\mathbf{k}'}$	$F_{\text{calc}}^{\mathbf{k}'}$	$h^{\mathbf{k}}$	$F_{\text{obs}}^{\mathbf{k}}$	$F_{\text{calc}}^{\mathbf{k}}$
-0.15	0.42	0.5	7.280	6.487	0.15	8.8130	8.2691
0.15	-0.42	0.5	7.550	6.206	-0.15	8.4691	8.2893
-0.15	-0.58	0.5	8.544	7.545	0.15	7.1362	6.8697
-0.15	-0.58	-0.5	8.602	6.892	0.15	7.2834	6.8684
-0.85	0.58	0.5	8.000	7.426	0.85	2.0599	1.1244
-1.15	0.42	-0.5	5.099	5.118	1.15	2.8397	4.2169
-1.15	-0.58	0.5	5.385	4.851	1.15	3.2573	3.9668
-0.85	-0.42	0.5	3.606	2.003	0.85	5.8267	6.0495
-1.85	-0.42	0.5	5.477	4.607	1.85	7.1667	6.4599
0.15	-0.42	-1.5	8.660	8.310	-0.15	8.8371	7.8371
0.15	-0.42	1.5	8.660	8.285	-0.15	8.5935	7.8208
-0.15	0.42	1.5	8.718	8.310	0.15	8.8130	7.8371
0.15	0.58	-1.5	11.747	12.104	-0.15	5.8990	5.1342
-0.15	-0.58	-1.5	11.874	12.058	0.15	5.9349	5.1453
-0.15	-0.58	1.5	11.662	12.104	0.15	6.4821	5.1342
-0.85	0.58	-1.5	6.000	6.474	0.85	2.0599	0.7765

most collinear with  $\alpha_{12}=13(3)^\circ$  ( $X=\text{Cl}$ ) and  $\alpha_{12}=22(4)^\circ$  ( $X=\text{Br}$ ), while the  $\text{Cu}_3\text{-Cu}_4$  arrangement is almost orthogonal  $\alpha_{34}=70(4)^\circ$  ( $X=\text{Cl}$ ) and  $\alpha_{34}=120(5)^\circ$  ( $X=\text{Br}$ ). Noting that the overlap between magnetic orbitals associated with the  $J_2$  path is almost zero<sup>8,9</sup> this might indicate that the intratetrahedral  $J_2$  coupling is rather weak. On the other hand, the angles between spins of different pairs in the same tetrahedron differ only slightly (see Table IV) and are close to  $145^\circ$  ( $X=\text{Cl}$ ) and  $120^\circ$  ( $X=\text{Br}$ ). These angles are the same for all tetrahedra in the structure and such regularity might imply that the  $J_1$  coupling mediated through the  $\text{Cu-O-Cu}$  superexchange path ( $\angle\text{Cu-O-Cu} \approx 110^\circ$ ) is strong.

Analysis of the angles between spins in adjacent tetrahedra reveals that neighboring ions across the  $[1 \pm 1 0]$  diagonals are almost antiparallel (Fig. 2 bottom). This implies that the intertetrahedral diagonal  $J_d$  coupling could be important with the linear superexchange path  $\text{Cu-X}\cdots\text{X-Cu}$  providing a strong AF interaction.<sup>8,9</sup> The angles between neighboring ions related by the  $[100]$  and  $[010]$  lattice translations are very different, in spite of the underlying tetragonal symmetry. One, for  $[100]$ , is acute ( $\alpha \approx 40^\circ$ ) and the other obtuse ( $\approx 140^\circ$   $X=\text{Cl}$ ,  $\approx 110^\circ$   $X=\text{Br}$ ) implying weak  $J_a$  and  $J_b$  coupling in accord with band-structure calculations.<sup>8</sup>

One further property of the proposed  $\mathbf{k}'$  spin arrangement should be discussed. This model leads to a finite resultant moment on each tetrahedron which is constant throughout the whole crystal. This moment rotates in the  $ac$  plane (Fig. 4) on a cycloid with the propagation vector  $(-k_x, 0, \frac{1}{2})$  giving

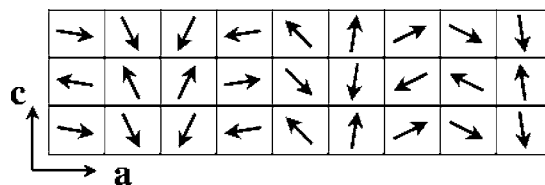


FIG. 4. The  $ac$  layer of resultant moment of tetrahedra of the  $\text{Cu}_2\text{Te}_2\text{O}_5\text{Cl}_2$   $\mathbf{k}'$  magnetic structure.

an angle of  $54^\circ$  ( $X=\text{Cl}$ ) and  $62^\circ$  ( $X=\text{Br}$ ) between the neighboring tetrahedra along  $a$ . Interestingly, the resultant moments on the tetrahedra in the chloride ( $0.333\mu_B$ ) and bromide ( $0.388\mu_B$ ) are almost equal, although the moment of the  $\text{Cu}^{2+}$  ions is close to the saturated value of  $1\mu_B/\text{Cu}$  for  $\text{Cu}_2\text{Te}_2\text{O}_5\text{Cl}_2$ , whereas it is significantly less for  $\text{Cu}_2\text{Te}_2\text{O}_5\text{Br}_2$ .

As the  $S=1/2$   $\text{Cu}^{2+}$  ion has very little single ion anisotropy, it is not clear what is responsible for the choice of the  $ac$  plane as the easy plane of the spins. It might be either the anisotropy of the intertetrahedral interactions or the DM interactions the direction of which is determined by the symmetry of the local environment.<sup>23</sup> The DM interaction could be nonzero in the  $\text{Cu}_2\text{Te}_2\text{O}_5\text{X}_2$  system and would give a DM vector in the  $ab$  plane<sup>24</sup> perpendicular to each  $\text{Cu-Cu}$  bond within the tetrahedra. This antisymmetric coupling would favor two spins to cant in opposite directions in the plane perpendicular to the DM vector and the fairly constant angle between nearest neighbor spins could reflect the ratio  $\text{DM}/J_1$ .

A thorough theoretical study is needed to clarify a number of questions raised by our findings.

(1) What relative strengths of the  $J_1$ ,  $J_2$  intratetrahedral and  $J_c$ ,  $J_d$ ,  $J_x$  (Ref. 20) intertetrahedral couplings are needed to give the experimentally observed  $\mathbf{k}'$  and  $\mathbf{k}$  structures.

(2) Can anisotropy of the intertetrahedral interactions alone explain the easy plane of the magnetic moments in the  $\mathbf{k}'$  structure.

(3) Does the choice of wave vector ( $\mathbf{k}'$  or  $\mathbf{k}$ ) determine the final spin arrangement adopted by the tetrahedra or do changes in strength of the  $J_1$ ,  $J_2$  couplings moderate the choice between the  $\mathbf{k}'$  (“canted coplanar”) and the  $\mathbf{k}$  (“canted pair”) structures.

## ACKNOWLEDGMENTS

This work was carried out at the ILL reactor, Grenoble, France and on SINQ at the Paul Scherrer Institute, Villigen, Switzerland. We would like to thank N. Kernavanois and M. Medarde for experimental assistance during the D3 experiment and A. M. Mulders for help during the X10 experiment. The sample preparation was supported by the NCCR research pool MaNEP of the Swiss NSF. S.J.C. acknowledges the financial support of the UK Engineering and Physical Sciences Research Council.

\*E-mail address: Oksana.Zaharko@psi.ch

- <sup>1</sup>*Magnetic Systems with Competing Interactions*, edited by H. T. Diep (World Scientific, Singapore, 1994).
- <sup>2</sup>M. Johnsson, K. W. Törnroos, F. Mila, and P. Millet, *Chem. Mater.* **12**, 2853 (2000).
- <sup>3</sup>P. Lemmens, K.-Y. Choi, E. E. Kaul, C. Geibel, K. Becker, W. Brenig, R. Valentí, C. Gros, M. Johnsson, P. Millet, and F. Mila, *Phys. Rev. Lett.* **87**, 227201 (2001).
- <sup>4</sup>J. Jensen, P. Lemmens, and C. Gros, *Europhys. Lett.* **64**, 689 (2003).
- <sup>5</sup>C. Gros, P. Lemmens, M. Vojta, R. Valenti, K.-Y. Choi, H. Kageyama, Z. Hiroi, N. V. Mushnikov, T. Goto, M. Johnsson, and P. Millet, *Phys. Rev. B* **67**, 174405 (2003).
- <sup>6</sup>M. Prester, A. Smontara, I. Zivkovic, A. Bilusic, D. Drobnic, H. Berger, and F. Bussy, *Phys. Rev. B* **69**, 180401(R) (2004).
- <sup>7</sup>A. V. Sologubenko, R. Dell'Amore, H. R. Ott, and P. Millet, *Eur. Phys. J. B* **42**, 549 (2004).
- <sup>8</sup>R. Valenti, T. Saha-Dasgupta, C. Gros, and H. Rosner, *Phys. Rev. B* **67**, 245110 (2003).
- <sup>9</sup>M.-H. Whangbo, H.-J. Koo, and D. Dai, *Inorg. Chem.* **42**, 3898 (2003).
- <sup>10</sup>W. Brenig and K. W. Becker, *Phys. Rev. B* **64**, 214413 (2001).
- <sup>11</sup>V. N. Kotov, M. E. Zhitomirsky, M. Elhajal, and F. Mila, *Phys. Rev. B* **70**, 214401 (2004).
- <sup>12</sup>S. J. Crowe, S. Majumdar, M. R. Lees, D. M. Paul, R. I. Bewley, S. J. Levett, and C. Ritter, *Phys. Rev. B* **71**, 224430 (2005).
- <sup>13</sup>O. Zaharko, H. M. Rønnow, A. Daoud-Aladine, S. Streule, F. Junanyi, J. Mesot, H. Berger, and P. J. Brown, *Fiz. Nizk. Temp.* **31**, 1068 (2005).
- <sup>14</sup>O. Zaharko, A. Daoud-Aladine, S. Streule, J. Mesot, P. J. Brown, and H. Berger, *Phys. Rev. Lett.* **93**, 217206 (2004).
- <sup>15</sup>Erratum to Ref. 14.
- <sup>16</sup>M. Blume, *Phys. Rev.* **130**, 1670 (1963).
- <sup>17</sup>S. V. Maleev, V. G. Bar'yaktar, and R. A. Suris, *Sov. Phys. Solid State* **4**, 2533 (1963).
- <sup>18</sup>P. J. Brown and J. C. Matthewman, *The Cambridge Crystallography Subroutine Library*, 1897.
- <sup>19</sup>P. J. Brown, *Physica B* **297**, 198 (2001).
- <sup>20</sup>Notations from Ref. 8 are adopted.
- <sup>21</sup>J. Rodriguez-Carvajal, *Physica B* **192**, 55 (1993).
- <sup>22</sup>S. Kirkpatrick, C. D. Gelatt Jr., and M. P. Vecchi, *Science* **220**, 671 (1983).
- <sup>23</sup>T. Morita, *Phys. Rev.* **120**, 91 (1960).
- <sup>24</sup>M. Elhajal and F. Mila (private communication).